Article

Cell Reports

Self-Antigen-Driven Thymic B Cell Class Switching Promotes T Cell Central Tolerance

Graphical Abstract

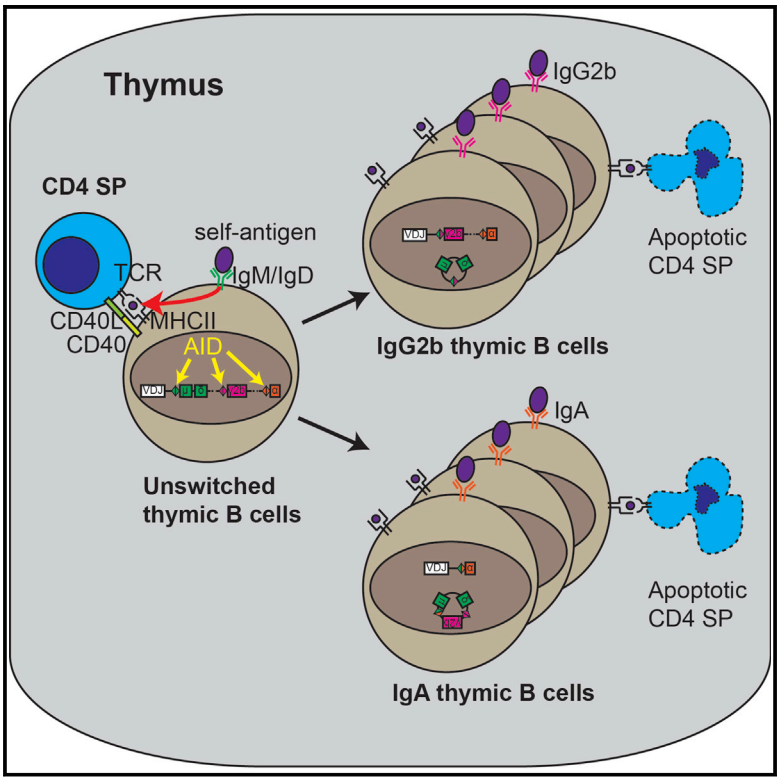

Authors

Jason Perera, Zhong Zheng, Shuyin Li, ..., Aaron R. Dinner, Martin Weigert, Haochu Huang

Correspondence

hhuang@bsd.uchicago.edu

In Brief

Perera et al. demonstrate that a large percentage of thymic B cells have undergone class switching intrathymically. Thymic B cell class switching requires cognate T-B interaction and is driven by self-antigens. These class-switched autoreactive thymic B cells play an important role in CD4 T cell tolerance.

Highlights

- A large percentage of thymic B cells undergo class switching intrathymically
- Thymic B cell class switching is dependent on cognate T-B interactions
- Class-switched thymic B cells have a distinct repertoire and are autoreactive
- $CD4^+$ T cells from $AID^{-/-}$ mice are autoreactive

Accession Numbers

GSE85366

Perera et al., 2016, Cell Reports *17*, 387–398
October 4, 2016
http://dx.doi.org/10.1016/j.celrep.2016.09.011

Cell Reports
Article

OPEN ACCESS
CellPress

Self-Antigen-Driven Thymic B Cell Class Switching Promotes T Cell Central Tolerance

Jason Perera,[1,2,8] Zhong Zheng,[2,8] Shuyin Li,[2] Herman Gudjonson,[1,3] Olga Kalinina,[4] Jennifer I.C. Benichou,[5] Katharine E. Block,[1,2] Yoram Louzoun,[6] Dengping Yin,[7] Anita S. Chong,[7] Aaron R. Dinner,[1,3] Martin Weigert,[1,4] and Haochu Huang[1,2,9,*]

[1]Committee on Immunology, University of Chicago, Chicago, IL 60637, USA
[2]Department of Medicine, Section of Rheumatology, and Knapp Center for Lupus and Immunology Research, University of Chicago, Chicago, IL 60637, USA
[3]Graduate Program in the Biophysical Sciences, Department of Chemistry, University of Chicago, Chicago, IL 60637, USA
[4]Knapp Center for Lupus and Immunology Research, Department of Pathology, University of Chicago, Chicago, IL 60637, USA
[5]The Mina and Everard Goodman Faculty of Life Sciences, Bar Ilan University, Ramat Gan 52900, Israel
[6]Department of Mathematics and Gonda Brain Research Center, Bar-Ilan University, Ramat Gan 52900, Israel
[7]Section of Transplantation, Department of Surgery, University of Chicago, Chicago, IL 60637, USA
[8]Co-first author
[9]Lead Contact
*Correspondence: hhuang@bsd.uchicago.edu
http://dx.doi.org/10.1016/j.celrep.2016.09.011

SUMMARY

B cells are unique antigen-presenting cells because their antigen presentation machinery is closely tied to the B cell receptor. Autoreactive thymic B cells can efficiently present cognate self-antigens to mediate CD4$^+$ T cell-negative selection. However, the nature of thymocyte-thymic B cell interaction and how this interaction affects the selection of thymic B cell repertoire and, in turn, the T cell repertoire are not well understood. Here we demonstrate that a large percentage of thymic B cells have undergone class switching intrathymically. Thymic B cell class switching requires cognate interaction with specific T cells. Class-switched thymic B cells have a distinct repertoire compared with unswitched thymic B cells or splenic B cells. Particularly, autoreactive B cell specificities preferentially expand in the thymus by undergoing class switching, and these enriched, class-switched autoreactive thymic B cells play an important role in CD4 T cell tolerance.

INTRODUCTION

Thymic B cells are a unique and highly effective antigen-presenting cell population within the thymic medulla (Klein et al., 2014; Perera and Huang, 2015). Together with conventional thymic dendritic cells, plasmacytoid dendritic cells, medullary thymic epithelial cells (mTECs), and macrophages they constitute a network of antigen-presenting cells (APCs) in the medulla that is responsible for removing autoreactive T cell specificities from the developing repertoire (Klein et al., 2014).

B cells are unique antigen-presenting cells because their antigen presentation machinery is closely tied to the B cell receptor (BCR). Antigens that are bound by the BCR are internalized and presented much more efficiently than by other APCs (reviewed in Lanzavecchia, 1990 and Yuseff et al., 2013). Therefore, the specificity of a B cell greatly influences the antigens it presents. We have shown that autoreactive thymic B cells can mediate T cell-negative selection efficiently (Perera et al., 2013). Although skewing the B cell repertoire toward a self-antigen greatly enhances negative selection, even the normal repertoire of thymic B cells is capable of presenting self-antigens for negative selection, suggesting that the thymic B cell repertoire may naturally contain autoreactive specificities. Still, little is known about how the thymic B cell repertoire is selected and regulated.

Phenotypically, thymic B cells express a number of costimulatory molecules such as CD80, CD86, and CD40 and increased levels of major histocompatibility complex (MHC) class II, which may facilitate their interaction with thymocytes (Ferrero et al., 1999; Perera et al., 2013). In the periphery, it is well established that cognate T-B interactions provide activating signals to the B cell partner, most notably through CD40, which, combined with BCR signals, results in proliferation, class switching, and antibody secretion (reviewed in Stavnezer et al., 2008 and Xu et al., 2012). Thymic B cells respond poorly to mitogens like lipopolysaccharide (LPS) or anti-immunoglobulin M (IgM) in vitro but can proliferate when cultured with MHC class II-restricted T cell blasts or anti-CD40 and interleukin-10 (IL-10) (Inaba et al., 1990, 1995). Although immature thymocytes lack the ability to mount a functional immune response, they do express costimulatory molecules, and CD4SP thymocytes in particular express CD40L (Desanti et al., 2012). CD40L expression on autoreactive CD4SP thymocytes has been shown to be critical for mTEC maturation, and, in their absence, mTECs fail to upregulate AIRE, CD80, and MHC class II (Desanti et al., 2012). Most recently, a similar effect has been described for thymic B cells, where CD40L signals promote AIRE expression and maturation in thymic B cells as well (Fujihara et al., 2014; Yamano et al., 2015). However, the nature of thymocyte-thymic B cell

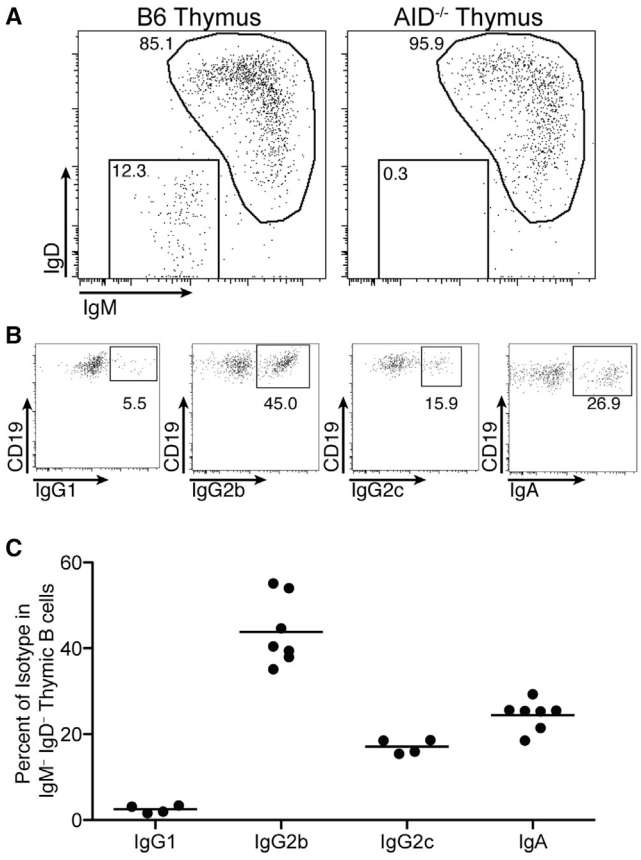

Figure 1. Detection of Class-Switched B Cells in the Thymus

(A) Staining of B6 or AID$^{-/-}$ thymus with anti-IgM and anti-IgD gated on B220^{+}Igκ^{+} cells.

(B) Expression of class-switched isotypes on CD19^{+}B220^{+}IgM^{-}IgD^{-} thymic B cells.

(C) Quantification of isotype usage by CD19^{+}B220^{+}IgM^{-}IgD^{-} thymic B cells. Shown is a representative of five independent experiments with four to seven mice per group.

interaction and how this interaction affects the selection of thymic B cell repertoire, and, in turn, the T cell repertoire is not well understood.

In this study, we show that a large proportion of murine thymic B cells undergo class switching. The presence of these class-switched thymic B cells is dependent on cognate interactions with thymocytes and activation-induced cytidine deaminase (AID). They possess a distinct B cell receptor repertoire with a massive expansion of autoreactive specificities, suggesting that autoreactive B cells are selected into the class-switched population and expanded within the thymus. Finally, CD4^{+} T cells from AID$^{-/-}$ mice show signs of increased autoreactivity, suggesting that thymic B cell class switching promotes CD4 T cell tolerance.

RESULTS

Identification of Class-Switched Thymic B Cells

Within the mature thymic B cell gate (CD19^{hi} B220^{hi}) we observed a population that did not express surface IgM or IgD and is composed 11%–33% of B cells (on average 18.5%) (Figure 1A). These cells were distinct from B220^{+}IgM^{-} thymic B cell progenitors that expressed lower levels of CD19 and B220 and were not included in this gate (Perera et al., 2013). Given that most of them expressed the kappa light chain, we hypothesized that this CD19^{hi}B220^{hi}IgM^{-}IgD^{-} population consisted of thymic B cells that had class-switched to downstream immunoglobulin isotypes. Flow cytometric analysis confirmed that the IgM^{-}IgD^{-} population was predominantly composed of B cells expressing the IgG2b (43.8%), IgA (24.4%), IgG2c (17.1%), or IgG1 (2.5%) isotypes (Figures 1B and 1C). We were unable to detect significant expression of IgG3 or IgE.

Class switching in B cells is critically dependent on AID, and AID$^{-/-}$ mice are deficient in all non-IgM classes of antibody (Muramatsu et al., 2000). We examined the thymi of AID-deficient mice and found that, although IgM^{+}IgD^{+} thymic B cells were unaffected, there was a complete absence of IgM^{-}IgD^{-} thymic B cells, confirming that this population is AID-dependent (Figures 1A and 4).

Class Switching Occurs Intrathymically

We next wanted to determine whether thymic B cells underwent class switch recombination intrathymically. Because AID is expressed during class switch recombination, we used AID-GFP reporter mice to identify AID-expressing cells in the thymus (Crouch et al., 2007). AID-GFP^{+} thymic B cells were predominantly found in the IgM^{-}IgD^{-} population, and the IgM^{-}IgD^{-} population had a distinct GFP profile (Figure 2A). When gated on the total pool of B cells in the thymus, we observed that 7.5% expressed GFP above the background set by the negative control (Figure 2B). This proportion was eight times higher than what was observed in the spleen and almost double what was seen in the mesenteric lymph node, which is a site of strong B cell activation and class switching in response to intestinal antigens (Figure 2C). Despite the increased frequency of AID-expressing cells, the expression level of AID was lower on a per-cell basis for thymic B cells, reaching only 24% of the median fluorescent intensity observed in AID-GFP^{+} cells in the spleen and 13% of the level observed in the mesenteric lymph node (Figures 2B and 2C). AID expression is known to vary at different anatomical sites and even between different regions of the germinal center, with cells in the dark zone expressing higher levels than cells in the light zone, although the functional significance of these differences is unknown (Crouch et al., 2007; Victora et al., 2012). The finding that class switching is lost in AID$^{-/-}$ mice (Figures 1A and 4) argues that the levels of AID observed in thymic B cells are sufficient to drive class switching. To further ascertain that AID expression in thymic B cells is active and functional, we assessed the presence of circle transcripts (CTs) in these cells. Class switching recombination is accompanied by deletion of circular DNA from the Ig heavy chain locus. Each circular DNA contains the I-promoter, which is still active in looped-out circular DNA and directs the production of I-Cμ transcripts termed CTs (Kinoshita et al., 2001). CTs are produced in an AID-dependent manner and disappear from B cells very rapidly. Thus, the presence of CTs is the best demonstration of active ongoing class switching. CTs for IgG2b (CT-γ2b), the most abundant isotype in thymic

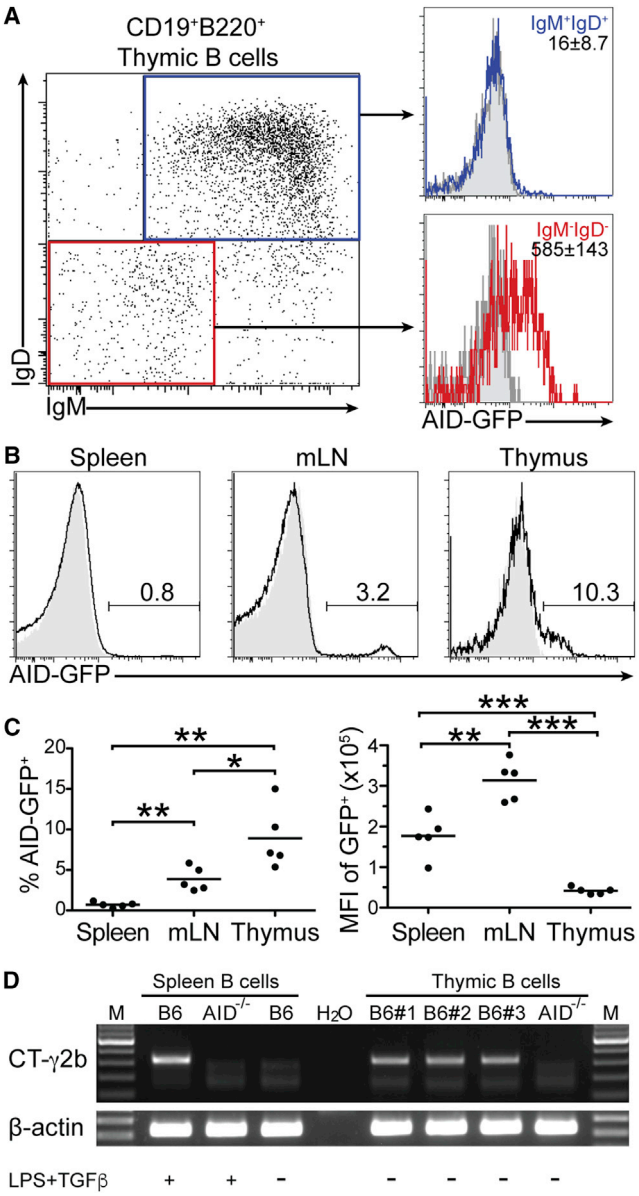

Figure 2. Detection of AID-GFP Reporter Expression in Thymic B Cells

(A) GFP expression in IgM^+IgD^+ and IgM^-IgD^- populations (gated on $B220^+$ $CD19^+$ cells) in the thymi of AID-GFP (open histograms) and WT control mice (gray histograms). Median fluorescence intensity (MFI) above background (with SD) is shown.

(B) Representative histogram showing the intensity of AID-GFP expression in the spleen, thymus, and mesenteric lymph node (mLN) in the $CD19^+B220^+$ population of AID-GFP (open histograms) and WT control mice (gray histograms).

(C) Quantification of the percentage and MFI of AID-GFP^+ cells in each organ as gated in (B). n = 5 mice representative of three experiments.

(D) Detection of CT-γ2b in thymic B cells. WT splenocytes stimulated with LPS and transforming growth factor β (TGF-β) were used as a positive control, and splenocytes or thymic B cells from $AID^{-/-}$ mice were used as a negative control. PCR products were verified by sequencing. Shown is a representative of two experiments.

B cells, were clearly detected in thymic B cells of wild-type (WT) B6 mice but not $AID^{-/-}$ mice (Figure 2D).

These data clearly demonstrate that there is active ongoing B cell class switching within the thymus, but they do not exclude the possibility that class switching in these cells is initiated in the periphery before they recirculate to the thymus. We previously demonstrated that B cells do not migrate from the blood into the thymus at a high frequency by generating parabiotic mice (Perera et al., 2013). To address whether class-switched thymic B cells might preferentially home to the thymus, we generated new parabiotic mice that had been joined for 6 weeks to examine the exchange of class-switched thymic B cells. In the first group, WT congenic CD45.1 and CD45.2 mice were joined (Figure 3A). Serving as controls, $CD4^+CD8^+$ thymocytes showed little exchange, whereas splenic B cells exchanged readily and reached an equilibrium of about 50%. Consistent with what we showed previously, about 25% of thymic B cells were derived from the parabiotic partner, and some proportion of this can be attributed to exchange of $B220^{lo}CD19^{lo}$ thymic B cell progenitors (Perera et al., 2013). Importantly, there is no significant difference in the level of exchange between thymic unswitched ($B220^{hi}$ $CD19^{hi}IgM^+IgD^+$) and class-switched B cells ($B220^{hi}CD19^{hi}IgM^-$ IgD^-), suggesting that there is no preferential recruitment of class-switched B cells to the thymus from the periphery (Figure 3B). Furthermore, the proportions of class-switched B cells to thymic B cells are the same regardless of whether they are host-derived or donor-derived, supporting that class switching takes place intrathymically (Figure 3C).

To further test whether there could be a niche for thymic class-switched B cells that may limit their exchange, we generated parabiotic mice with WT (CD45.1) and $AID^{-/-}$ (CD45.2) mice (Figure 3D). The levels of exchange of unswitched thymic B cells were similar in WT or $AID^{-/-}$ partners (Figure 3E). Because $AID^{-/-}$ mice are defective in class switching, there would be no pre-existing class-switched thymic B cells to occupy such a niche. WT thymic class-switched B cells in $AID^{-/-}$ mice after joining with a WT partner could be due to two possible events: unswitched WT B cells recirculate to the thymus of the $AID^{-/-}$ partner and class-switch intrathymically, or WT pre-existing class-switched B cells recirculate to the thymus of the $AID^{-/-}$ partner. If the latter is the main source of thymic class-switched B cells, one would predict that both WT and $AID^{-/-}$ partners should have the same numbers of thymic class-switched B cells or that the proportion of class-switched thymic B cells to unswitched thymic B cells would be much higher in the $AID^{-/-}$ partners. Our analyses showed that this was not the case. The proportion of thymic class-switched B cells to non-switched B cells in $AID^{-/-}$ partners was the same as that of WT partners (Figure 3F), and there were significantly fewer class-switched thymic B cells in $AID^{-/-}$ partners than in WT partners (Figure 3F). Taken together, all of these data demonstrate that thymic B cell class switching occurs intrathymically.

Class Switching Requires Interactions with Specific T Cells

Next, we addressed the requirements for class switching in thymic B cells. We found that cognate interactions with developing thymocytes were critical for thymic B cell class switching

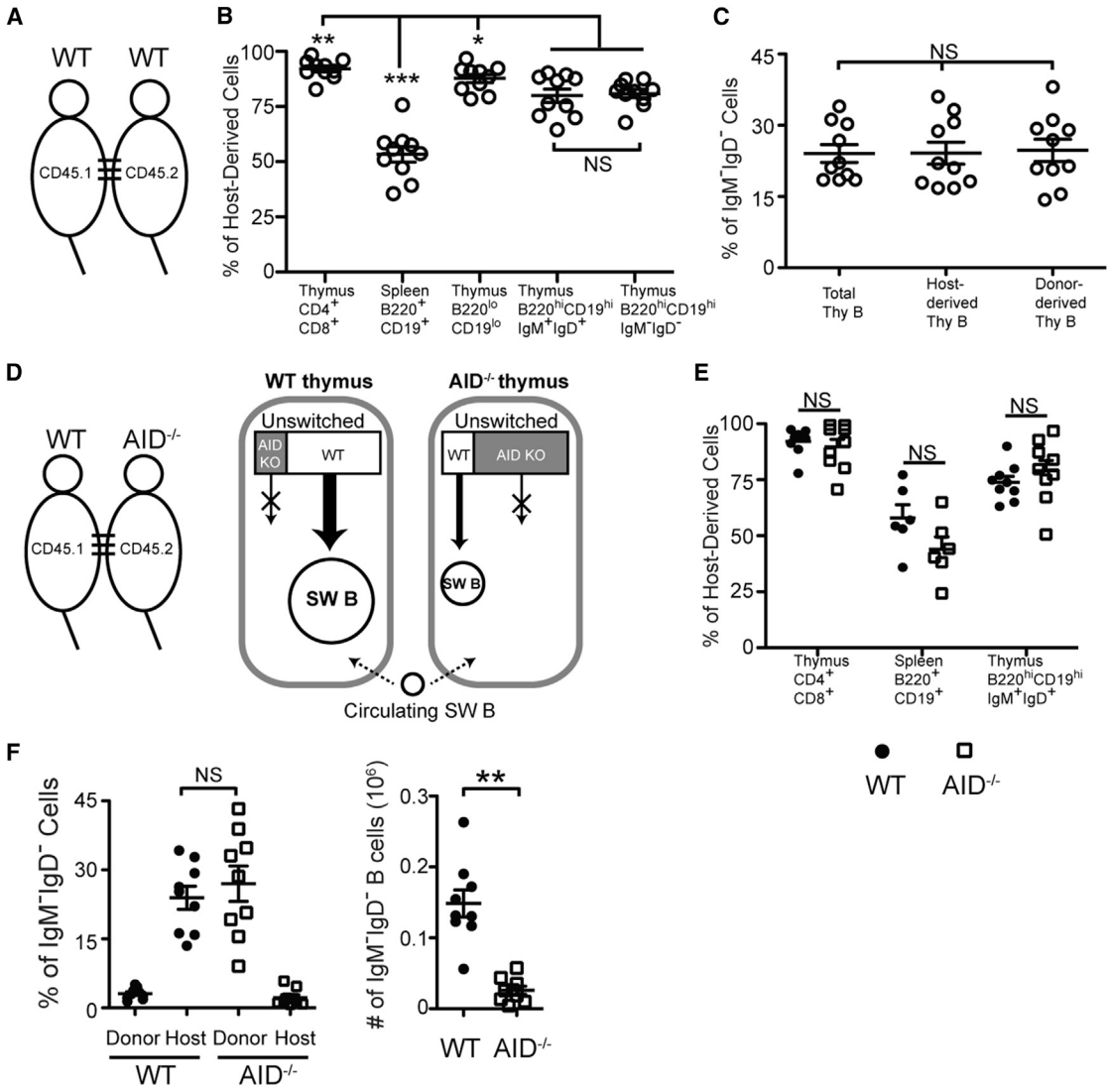

Figure 3. The Exchange of Class-Switched Thymic B Cells following 6-Week Parabiosis

(A) Parabiotic partners of WT mice. Analyses of the parabiotic partners were combined and are shown in (B) and (C).

(B) Quantification of the percentage of host-derived cells in various cell B cell populations. Host-derived cells were determined by staining with antibodies for CD45.1 and CD45.2. Each symbol represents one individual mouse. n = 10.

(C) Percentage of class-switched B cells in thymic B cells (total, host-derived, and donor-derived, respectively).

(D) Parabiotic partners of WT and AID$^{-/-}$ mice and potential sources of thymic B cells. Analyses of WT and AID$^{-/-}$ partners are shown separately in (E) and (F).

(E) Quantification of the percentage of host-derived cells in various cell populations. Each symbol represents one individual mouse. n = 9 from two experiments.

(F) Percentage of class-switched B cells in host-derived or donor-derived thymic B cells in parabiotic partners (left). Also shown is the total number of class-switched thymic B cells in parabiotic partners (right).

Mean ± SEM of each data group is shown.

(Figure 4). T cell receptor (TCR)$\alpha^{-/-}$ mice completely lacked class-switched thymic B cells, demonstrating a requirement for mature thymocytes. Expression of MHC class II on thymic B cells was also essential because class switching was greatly reduced when the floxed first exon of I-A^b (Hashimoto et al., 2002) was conditionally deleted in B cells using Mb1-Cre (Hobeika et al., 2006). To test whether TCR specificity was important, we used OT-II mice that possessed a greatly restricted TCR repertoire toward the non-self-antigen ovalbumin (Barnden et al., 1998). This restriction of T cell specificity led to a dramatic reduction in thymic B cell class switching, suggesting that class switching requires cognate interaction between thymocytes and thymic B cells. The residual class switching observed in OT-II mice could be explained by the presence of a small population of thymocytes with endogenously rearranged TCRs capable of recognizing self-antigens on thymic B cells (Yamano et al., 2015). In addition, we found that CD40 deficiency also dramatically reduced class switching, further emphasizing the importance

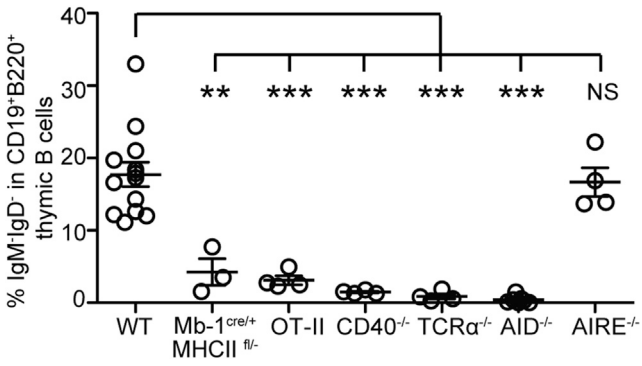

Figure 4. Requirements for Thymic B Cell Class Switching

Shown is the quantification of the percentage of $IgM^{-}IgD^{-}$ cells within the $CD19^{+}B220^{+}$ thymic B cell gate. Statistical analysis was performed using Student's t test. n = 3–8 mice/group. Shown are data from ten independent experiments.

Mean ± SEM of each data group is shown.

of thymocyte-B interactions in driving this phenomenon. Finally, we examined whether AIRE is required for class switching because AIRE is induced in thymic but not peripheral B cells (Yamano et al., 2015). As shown in Figure 4, we found no significant difference in thymic B cell class switching in *Aire*$^{-/-}$ mice, suggesting that AIRE is not essential for class switching.

Class-Switched Thymic B Cells Have a Distinct Repertoire

The fact that thymic B cell class switching was dramatically reduced in OT-II mice suggested that autoreactive T cell specificities were critical for driving class switching in the thymus. Studies on germinal center responses demonstrate that germinal center B cells compete for T cell help and that B cells with higher affinity for cognate antigen get preferential help, which is essential for establishing specificity in germinal center response (Victora et al., 2010). We next wanted to determine whether B cell specificity was also important for class switching in the thymus. We reasoned that, if BCR signaling and/or the ability to bind and present self-antigen to T cells drives class switching, then the BCR repertoires of switched B cells should be distinct from unswitched B cells in the thymus. To test this, we took advantage of the 3H9 model of anti-DNA reactivity, which is a well-studied system for understanding tolerance in B cells. The 3H9 heavy chain predisposes the B cell receptor toward anti-DNA reactivity while also allowing for binding to single-stranded DNA (ssDNA), purified nucleosomes, cardiolipin, and phosphatidylserine (Cocca et al., 2001; Radic et al., 1991). The 3H9 transgenic mice exhibit excellent heavy-chain allelic exclusion, and the contribution of endogenous light chains to 3H9 binding specificities is well characterized, facilitating analysis of alterations in the polyclonal repertoire. On a nonautoimmune-prone background, light chains that retain 3H9's anti-DNA specificity lead to developmental arrest and receptor editing in the bone marrow, whereas light chains that can "edit" the anti-DNA reactivity of the 3H9 heavy chain allow B cells to develop further (Gay et al., 1993). This approach has been applied previously to study how BAFF regulates the B cell repertoire (Ota et al., 2010).

We performed high-throughput sequencing (HTS) analysis of the light chain repertoire of class-switched thymic B cells ($CD19^{+}$ $B220^{+}$ IgM^{-} IgD^{-}), unswitched thymic B cells ($CD19^{+}$ $B220^{+}$ IgM^{+} IgD^{+}), and bulk splenic B cells in 3H9 mice. On average, we sorted 26,500 IgM^{+} IgD^{+} thymic B cells, 8,700 IgM^{-} IgD^{-} thymic B cells, and 3.7×10^{6} splenic B cells with a sequencing depth ranging from 2.2×10^{5} to 3.5×10^{6} total reads per sample. Our sequencing strategy provided us with sequences that spanned CDR3, including the entirety of the Jκ and 66 base pairs (bp) of the Vκ FR3 region, which allowed us to accurately identify the V family and, in the majority of cases, the specific Vκ gene. Our sequencing covered a broad range of Igκ families, although certain Igκ families (Vκ2, Vκ12, Vκ13, and Vκ15) were under-represented because of mismatches of the PCR forward primer with these particular V genes. This potential bias, inherent to any multiplex PCR-based sequencing strategy, makes absolute determination of the abundance of Igκ families within each sample difficult. However, because these primer biases affect all samples equally, comparing the relative abundance of an Igκ family between samples is quite reliable, reflected by the small variation in Igκ V family usage between different mice within a group. This consistency is particularly evident in the spleen, where the larger number of input cells reduced the potential for sampling bias. From these data, we were able to identify unique V-J-CDR3 amino acid combinations and track their relative abundance between samples.

To first identify broad differences, we focused on unique V-J-CDR3 amino acid combinations that reached an abundance of at least 0.1% in any sample (460 of 22,000 unique combinations that accounted for about 90% of reads in each sample) and performed principal component analysis on them, as described in the Experimental Procedures. We found that PC1 and PC2 segregated the three populations (Figure 5A). Specifically, we observed that PC1 distinguished class-switched samples from unswitched thymic and splenic B cell samples, whereas PC2 further distinguishes splenic samples from unswitched thymic B cell samples.

Next, we measured the similarity between sample repertoires using the Morisita-Horn dissimilarity index. This statistic sums over the overlaps (products) of BCR sequence read counts, scaled by a measure of the diversity within each sample: 1 as completely different and 0 as identical. Although the splenic and thymus unswitched replicates were internally similar to one another (i.e., spleen versus spleen, $IgM^{+}IgD^{+}$ versus $IgM^{+}IgD^{+}$), there was a large and variable dissimilarity among the switched thymic B cell replicates ($IgM^{-}IgD^{-}$ versus $IgM^{-}IgD^{-}$), suggesting that their repertoires were less uniform (Figure 5B). There was also a large dissimilarity between the unswitched, switched, and splenic B cell samples. Together with the principal component analysis, these findings indicated that thymic $IgM^{+}IgD^{+}$, thymic $IgM^{-}IgD^{-}$, and splenic B cells all possessed distinct B cell repertoires.

When we compared light chain family usage between groups, we observed a dramatic expansion of Vκ5 family (sometimes referred to in the literature as Vκ23) usage in the $IgM^{-}IgD^{-}$ thymic B cell repertoire (Figures 5C and 5D). This expansion came largely from an increase in the number of sequences from the 5-43/5-45 genes, whereas the majority of the expression

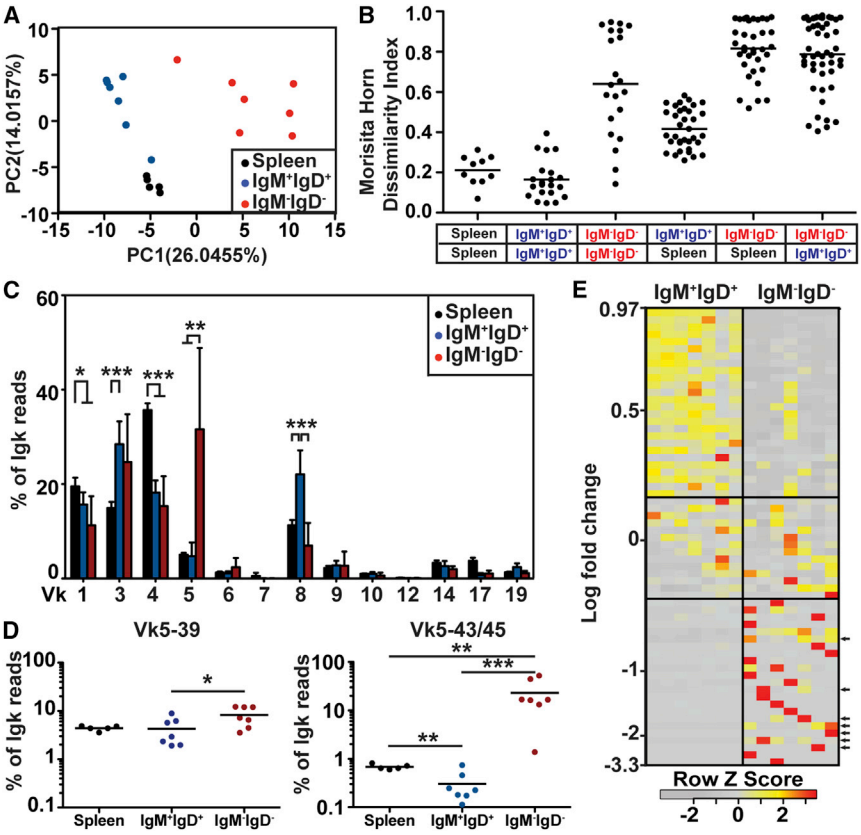

Figure 5. Analysis of the Light Chain Repertoire in Thymic B Cell Populations in 3H9 Transgenic Mice

(A) PCA of light chains for splenic (black), IgM^+IgD^+ thymic (blue), and IgM^-IgD^- thymic (red) B cells.

(B) Morisita-Horn dissimilarity index comparing the dissimilarities between the indicated groups.

(C) Vκ gene family usage in splenic, IgM^+IgD^+, and IgM^-IgD^- thymic B cells from 3H9 mice. Relative usage of each Vκ family (the percentage) is calculated as the number of productive reads attributed to that family divided by the total number of productive Igκ reads for each sample. The mean and SD of values for each population are plotted. Statistical analysis was performed by Mann Whitney *U* test. n = 5–7 mice/group.

(D) Relative usage of the Vκ 5-39 and Vκ 5-43/45 families. Each dot represents one mouse. Statistical analysis was performed by Mann Whitney *U* test.

(E) Heatmap of the relative usages of the most abundant light chains (>1% of the repertoire) in each mouse sample, sorted by log fold change in abundance between thymic IgM^+IgD^+ and IgM^-IgD^- populations. Black arrows indicate sequences using Vκ 5-43/45.

observed in the spleen and IgM^+IgD^+ compartment comes from the 5-39 family. In addition, both thymic B cell subsets had reduced usage of Vκ4 and Vκ1 as well as increased usage of Vκ3 relative to splenic B cells. One unique feature of the thymic IgM^+IgD^+ repertoire was its increased usage of Vκ8 compared with the other two B cell repertoires (Figure 5C).

In-depth analysis of individual BCRs confirmed the broad difference observed between the thymic IgM^+IgD^+ and IgM^-IgD^- repertoires and provided more insights. Within the IgM^+IgD^+ repertoire, the most highly abundant BCRs were shared among all replicates, whereas the BCRs that were highest in the IgM^-IgD^- repertoire were more variable, and most were expressed in only one or two mice, confirming the analysis with the Morisita-Horn index (Figure 5E). Also, these unique BCRs were greatly expanded, and sometimes a single BCR accounted for up to 45% of the total Igκ reads (Figures 5E and 6A). Finally, a large proportion of the most highly expressed and highly overrepresented BCRs in the IgM^-IgD^- repertoire came from the Vκ5 family (Figure 5E, black arrows), confirming the analysis of Vκ usage shown in Figure 5C. These results confirm that there are consistent and substantial differences between the repertoires of IgM^+IgD^+ and IgM^-IgD^- thymic B cells and further suggested that BCR specificity was a contributing factor to class switching.

Mutation Frequency in Thymic B Cells

In addition to class switch recombination, AID expression also drives somatic hypermutation. To determine whether there was accumulation of mutations in thymic B cells, we compared mutation frequencies between the three repertoires. The junctional diversity introduced during recombination made tracking mutations around CDR3 difficult, so we limited our analysis to the region directly upstream, which includes approximately 50 bp of the FR3 region. Although we found a slight increase in the proportion of BCRs containing a single mutation in the switched repertoire (up to 4.2% from 0.1%), we did not observe signs of accumulated somatic hypermutation (Figure S1A). As a further confirmation, we analyzed full-length BCR sequences of light chains cloned from the IgM^+IgD^+ and IgM^-IgD^- repertoires (60 sequences from each repertoire). Although the overall mutation frequency was higher, presumably because of higher PCR and sequencing errors generated by much longer templates, there was no difference in mutation frequency for the two populations (Figure S1B). The lack of mutations in light chains was not an artifact of the 3H9 transgenic mice because germinal center B cells isolated from mesenteric lymph nodes of these mice showed significant numbers of mutations (Figure S1C). These results suggest that AID's class switch recombination and somatic hypermutation functions are differentially regulated in thymic B cells.

Antibodies Generated from Switched B Cells Are More ANA-Reactive

The repertoire analyses supported our hypothesis that unique BCR specificities were driven to class-switch by self-antigens. It is striking to note that the Vκ5 light chain family was found to be expanded in 3H9 mice on autoimmune-prone backgrounds such as MRL/lpr and NZW/BXSB.Yaa and almost absent in the

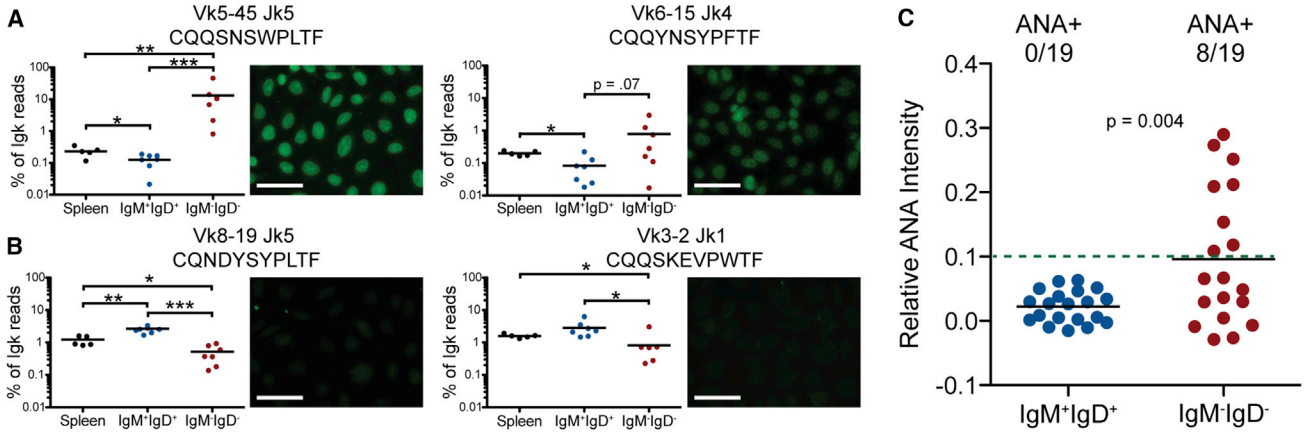

Figure 6. Relative Usage and Reactivity of Differentially Represented BCRs

(A) Relative abundance of specific Vκ5 and Vκ6 BCRs (CDR3 sequences are shown) that are consistently upregulated in $IgM^{-}IgD^{-}$ thymic B cells and representative ANA staining by the same antibodies expressed in vitro. Scale bar, 50 μm.

(B) Relative abundance of specific Vκ8 and Vκ3 BCRs (CDR3 sequences are shown) that are consistently upregulated in $IgM^{+}IgD^{+}$ thymic B cells with representative ANA staining.

(C) Quantification of the relative intensity of nuclear staining. The frequency of ANA^{+} antibodies is shown on top. n = 19 antibodies/group.

repertoires of healthy mice (Chen et al., 2006; Moisini et al., 2012). To test whether these BCRs were autoreactive and compare them with BCRs from the non-switched thymic B cells, the full-length cDNA of the most abundant V-J-CDR3 sequences observed in the $IgM^{+}IgD^{+}$ and $IgM^{-}IgD^{-}$ thymic B cell repertoires were amplified and cloned (Figure 5E). We then expressed these light chains together with the 3H9 heavy chain in vitro and tested their reactivity to nuclear antigens by staining HEp2 cells. Examples of such specific BCRs from the $IgM^{+}IgD^{+}$ and $IgM^{-}IgD^{-}$ thymic B cell repertoires and corresponding antinuclear antibody (ANA) staining are shown in Figures 6A and 6B, respectively. Altogether, we expressed 19 BCRs from the $IgM^{+}IgD^{+}$ repertoire and 19 from the $IgM^{-}IgD^{-}$ repertoire that covered 26.2% and 42.6% of the total Igκ reads for each population, respectively. Quantification of the relative intensity of nuclear staining showed no positive anti-nuclear staining from any of the $IgM^{+}IgD^{+}$ BCRs, but 8 of 19 $IgM^{-}IgD^{-}$ BCRs displayed significant ANA staining over background (Figure 6C). These ANA-positive BCRs were predominantly from the Vκ5 family (seven of eight), with one being derived from the Vκ6 family, and the contribution of these eight autoreactive BCRs accounted for 23.9% of the Igκ reads from $IgM^{-}IgD^{-}$ thymic B cells.

Thymic B Cell Class Switching Regulates the T Cell Repertoire

We have shown that autoreactive thymic B cells are excellent APCs for T cell-negative selection (Perera et al., 2013). Because class-switched thymic B cells are enriched with autoreactivity, we hypothesized that they contributed to T cell-negative selection. Furthermore, we would predict increased T cell autoreactivity in mice where class switching was absent. To determine how T cell autoreactivity is affected, we adapted a CD4 T cell transfer protocol that has been used previously to measure autoreactivity within the T cell repertoire (Yamano et al., 2015). In this approach, polyclonal T cells are adoptively transferred into congenic hosts, and their proliferation and differentiation are measured. WT CD4 T cells transferred into B6 congenic hosts should proliferate minimally because they are already tolerant of all antigens in the new host. However, T cells from a host with defective central tolerance should proliferate more extensively because they will be encountering antigens to which they have not been tolerized previously.

We purified $CD4^{+}$ T cells from the spleens of B6 or $AID^{-/-}$ mice and carboxyfluorescein succinimidyl ester (CFSE)-labeled and injected them intravenously (i.v.) into CD45.1 congenic B6 recipient hosts. 7 days after transfer, we observed twice as many $CFSE^{lo}$ cells in the $AID^{-/-}$ $CD4^{+}$ T cells relative to wild-type controls, indicating that they contained more autoreactive cells and/or had proliferated more extensively (Figure 7). This increased proliferation also corresponded with a doubling of the proportion of transferred cells that upregulated the follicular helper T cells (Tfh) markers PD1 and CXCR5, suggesting that their activation was coupled to differentiation into a T effector phenotype (Figure 7).

DISCUSSION

In this study, we show that thymic B cells undergo class switching intrathymically in response to their interactions with developing thymocytes. These interactions are driven by self-antigens based on the loss of class switching in OT-II mice and the enrichment of autoreactive specificities in the class-switched thymic B cell repertoire. Furthermore, when class switching is inhibited, the T cell repertoire shows signs of increased autoreactivity. Together with previous studies, our findings support a model where thymic B cells couple a broad recognition of self-antigens with an enhanced antigen presentation capacity to purge cognate T cells from the developing repertoire.

How can one reconcile the two seemingly contradictory roles for autoreactive thymocytes in this model: autoreactive

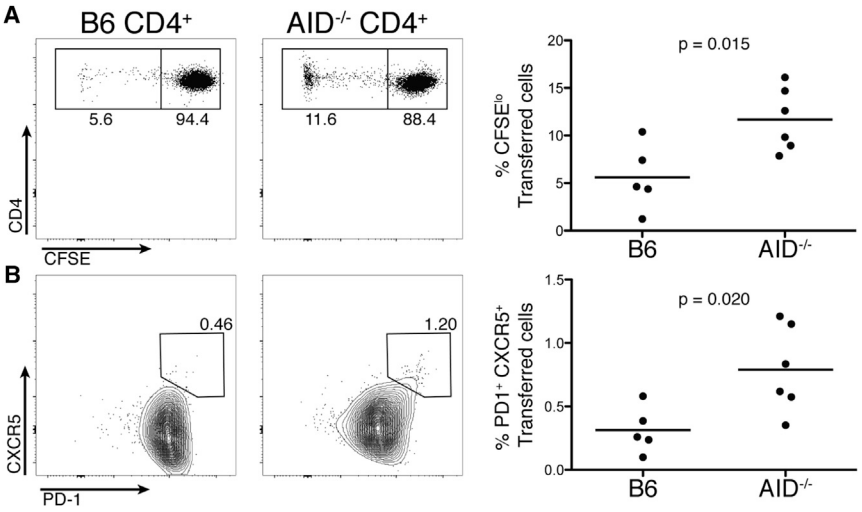

Figure 7. Increased Self-Reactivity in the CD4$^+$ T Cell Compartment of AID$^{-/-}$ Mice

(A) CD4$^+$ T cells from B6 or AID$^{-/-}$ mice were adoptively transferred into CD45.1 congenic hosts. 7 days later, donor cells in lymph nodes were analyzed, and representative CFSE dilution and Tfh staining are shown (gated on CD45.2$^+$CD4$^+$ cells).

(B) Quantification of CFSE^{lo} cells and Tfh cells as shown in (A). Shown is a representative of four independent experiments. n = 5–6 mice/group.

thymocytes drive thymic B cell class switching and autoreactive thymocytes undergo negative selection in response to these interactions? Although the outcome of cognate interactions for autoreactive thymocytes with various APCs is apoptosis or lineage conversion to regulatory T (Treg) cells, this process does not occur immediately. Two-photon microscopy of the thymic medulla shows that, following antigen encounter, autoreactive thymocytes narrow their migration but still remain active for hours after antigen exposure, allowing for potentially meaningful interactions with negatively selecting APCs (Le Borgne et al., 2009). This mode of interaction between thymocytes and cognate B cells is analogous to a negative feedback loop that serves to keep autoreactive thymocytes in check. It helps to "focus" the antigen presentation of thymic B cells to the most relevant specificities—a safeguard to prevent the accidental escape of autoreactive T cells considering the random nature of T cell and APC encounters in the thymus.

The expansion of Vκ5 family members in 3H9 thymic class-switched B cells (sometimes referred to in the literature as Vκ23) is particularly interesting because this light chain has been linked to the generation of highly autoreactive anti-DNA antibodies when paired with the 3H9 heavy chain. The Vκ5-43 and 5-45 genes are rarely detected in non-autoimmune mice, but their over-representation is common among anti-DNA antibodies in different autoimmune mice (Brard et al., 1999; Chen et al., 2006; Liang et al., 2003; Moisini et al., 2012; Roark et al., 1995; Tillman et al., 1992). Although a common property of editor light chains is the presence of negatively charged residues within CDR1 and 2, Vκ5-43 and 5-45, in contrast, have positively charged arginines in these regions, leading to the suggestion that they may confer a selective advantage to anti-DNA antibodies in diseased mice when cognate T cell help is present in an autoimmune-prone genetic background (Chen et al., 2006). The amplification and enrichment of these kinds of B cells in the thymus would pre-empt the development of such T cells in normal mice. Another member of the Vκ5 family, Vκ5-39, can be detected in the normal repertoire and is only marginally enriched in class-switched thymic B cells (Figure 5D). This could be due to a unique aspartic acid residue in CDR1 that is negatively charged and might counteract the arginine residues.

It is important to note that B cell antigen presentation is fundamentally distinct from other APCs. Although dendritic cells and macrophages acquire the bulk of their antigens from phagocytosis, pinocytosis, macropinocytosis, and receptor-mediated endocytosis, B cells do not perform these processes efficiently and, instead, take up antigen almost exclusively via their B cell receptor (Watts, 1997). Thus, B cell specificity dictates the antigens that are presented by B cells. Antigen-specific B cells effectively present their cognate antigens at 1,000 times lower concentrations than non-cognate antigen, allowing them to activate cognate T cells when antigen concentrations are well below the K_d of the antibody (Lanzavecchia, 1990). Antigen-specific B cells can also present antigens at 100 times lower concentrations than dendritic cells in vivo (Pape et al., 2007). Another factor to consider is that, even when the pool of antigens is the same, the processing of peptides by B cells could be distinct from other thymic APCs. Antibody binding can protect peptide epitopes from degradation so that B cells binding two different epitopes on the same antigen can produce very different antigen digestion patterns (Davidson and Watts, 1989).

In light of these unique properties, the non-redundant function of thymic B cells may lie in their capacity to diversify the pool of self-peptides that are presented to developing thymocytes. For cases like the anti-DNA 3H9/Vκ5 B cells that we report here, the antigens presented by these B cells would likely be proteins that are associated with DNA, such as histones. Apoptotic cells are considered the source of DNA, histones, and nucleoprotein complexes. DNA and nucleosomes have been demonstrated to be associated with the cell surface of apoptotic cells (Casciola-Rosen et al., 1994; Radic et al., 2004), although the exact nature of DNA accessible to BCR is still not well understood. Given the ability of 3H9 to bind phosphatidylserine and the fact that phosphatidylserine would be present on abundant apoptotic thymocytes, it is possible that 3H9/Vκ5 B cell activation and class switching are driven by self-antigens contained in apoptotic blebs. In addition, peptides derived from immunoglobulin as well as B cell-specific antigens may also be preferentially presented by thymic B cells (Perera and Huang, 2015). TCR transgenics that recognize immunoglobulin determinants are subject to enhanced negative selection when B cells with the

corresponding BCRs are present in the thymus (Detanico et al., 2011; Rudensky et al., 1990). Furthermore, B cells are the dominant cell type presenting immunoglobulin peptides in the thymus, with very little contribution from other thymic APCs (Rudensky et al., 1990). T cells that are specific for BCR peptides can become pathogenic when they escape into the periphery (Detanico et al., 2011; Munthe et al., 2005). In these cases, BCR autoreactivity is not required per se, but the specificity of the T-B interaction still relies on dominant presentation of cognate antigen by specific B cells.

A recent paper by Yamano et al. (2015) describes a process that they call thymic B cell licensing. Licensing is characterized by MHC II and CD80 upregulation, induction of AIRE, and class switching in a portion of $AIRE^+$ B cells (about a quarter to a third). Expression of AIRE allows thymic B cells to express a unique set of tissue-restricted antigens. They argue that thymic B cell licensing is independent of BCR autoreactivity. This conclusion is drawn from two experiments. In the first experiment, SW_{HEL} mice are used in which a majority of the B cells express a BCR that is specific for the non-self-antigen hen egg lysozyme (HEL). In these mice, HEL-binding B cells upregulate MHC II and CD80 and class-switch with a similar frequency as non-HEL-binding B cells. Nonetheless, their data could be interpreted by two alternatives that are compatible with our model: allelic inclusion of autoreactive specificity in HEL-binding B cells could be responsible for their switching, and SW_{HEL} BCR itself may contain epitopes that are recognized by the endogenous T cell repertoire. In the second experiment, they show that BCR simulation counteracts AIRE induction, suggesting that thymic B cell licensing is independent of BCR stimulation. However, as shown by their bone marrow chimera data that *Aire*$^{-/-}$ thymic B cells have a very slight decrease in class switching, we confirmed that *Aire*$^{-/-}$ mice have no defects in thymic B cell class switching (Figure 4).

Each B cell displays many peptides on its surface that, by definition, are all autoantigens, and a large number of peptides are derived from self-cytosolic proteins (Dongre et al., 2001). Clearly these peptides are not acquired through internalization of autoreactive BCRs. However, the issue is the relative efficiency of presentation. When BCR recognizes the specific autoantigen, the B cell presents autoantigen much more efficiently than bulk B cells and is preferentially selected for T cell help. The preferential selection of autoreactive specificities in the class-switched thymic B cells is analogous to germinal center B cell selection in autoimmunity. Yamano et al. (2015) proposed that resting B cell antigens are responsible for thymic B cell licensing and allow thymic B cells to present activated B cell antigens and AIRE-dependent antigens. Our model suggests that class-switched thymic B cells have a unique bias toward auto-reactive BCRs and target the negative selection of certain autoreactive thymocytes. Taken together, these results suggest that thymic B cell licensing is BCR-independent, whereas class switching is BCR-dependent.

It has been shown that ectopically transferred B cells can home to the thymus (Akashi et al., 2000; Yamano et al., 2015). However, it is an inefficient process, and only a small percentage of transferred cells can be detected in the thymus. Parabiosis allows us to test the contribution of peripheral B cells in a physiological setting over an extended period. These experiments demonstrate that imported peripheral B cells make only a minor contribution, even more so in light of the similar import of B cell progenitors ($B220^{lo}CD19^{lo}$) in the thymus. Our repertoire analysis of unswitched splenic versus thymic B cells showed that they are distinct, further supporting that they develop in the bone marrow versus thymus, respectively.

The cytoplasmic regions of class-switched immunoglobulins (Igs) are much longer than those of IgM and IgD and are evolutionarily conserved. The IgG cytoplasmic tails contain a conserved YXXM amino acid motif that functions as an internalization signal for antigen processing and presentation. Using transgenic mice expressing antigen-specific IgM, IgG, or a chimeric IgM with the IgG cytoplasmic tail, Martin and Goodnow (2002) showed that the IgG tail greatly enhanced the survival of progeny cells, leading to expanded numbers. Thus, the class switching of autoreactive thymic B cells could have important biological implications for their function as APCs in T cell tolerance. Our results on T cell tolerance defects in $AID^{-/-}$ mice is consistent with earlier findings that AID deficiency in both mice and humans results in autoimmunity (Chen et al., 2010; Hase et al., 2008; Kuraoka et al., 2011; Meyers et al., 2011). Future studies will be needed to determine the exact contribution of thymic class-switched B cells in shaping the T cell repertoire.

EXPERIMENTAL PROCEDURES

Mice

$AID^{-/-}$ (Muramatsu et al., 2000), AID-GFP (Crouch et al., 2007), Mb1-Cre (Hobeika et al., 2006), $I\text{-}A^{fl/fl}$ (Hashimoto et al., 2002), OT-II (Barnden et al., 1998), $CD40^{-/-}$ (Kawabe et al., 1994), $AIRE^{-/-}$ (Anderson et al., 2002), and 3H9 (Chen et al., 1995) mice were described previously. Unless otherwise stated, 6- to 12-week-old mice were used in the experiments. All mice were housed in a specific pathogen-free facility, and the experiments were approved by the University of Chicago Institutional Animal Care and Use Committee.

Antibodies and Flow Cytometry

Monoclonal antibodies for flow cytometry against mouse B220 (RA3-6B2), CD19 (ebio1D3), CD45.2 (104), CD45.1 (A20), IgM (11/41), IgD (11-26), CD4 (RM4-5), CD8 (53.6.7), IgG1(A85-1), IgG2b (RMG2b-1), IgG2c, and IgA (Southern Biotech), were purchased from eBioscience, BD Biosciences, and BioLegend or provided by the Fitch Monoclonal Antibody Facility at the University of Chicago. Samples were collected on a FACSCanto (BD Biosciences), and data were analyzed using FlowJo (Tree Star). Cell sorting for 3H9 class-switched versus unswitched populations was performed on a FACSAria (BD Biosciences).

Analysis of Thymic B Cells

Thymi were dissected carefully to avoid the parathymic lymph nodes. Thymic B cells were enriched by either depleting bulk thymocytes with anti-CD4 (GK1.5) and anti-CD8 (2.43.1) or by positive selection with anti-B220 (RA3-6B2) using MACS microbeads (Miltenyi Biotec).

Circle Transcript Detection

Mouse thymic B cells were purified from thymocytes using EasySep beads (STEMCELL Technologies) to deplete non-B cells with an antibody cocktail containing biotin-labeled anti-mouse CD4, CD8, Gr-1, Ter119, CD11c, CD11b, and NK1.1. Total RNA was isolated from thymic B cells using the RNA microprep kit (Zymo Research). cDNA was synthesized with ProtoScript II reverse transcriptase (New England Biolabs) using 250 ng of total RNA and poly $d(T)_{18}$. $I\gamma 2b\text{-}C\mu$ transcripts were amplified by two rounds of nested PCR. The primers for the first round of PCR were as follows: 5′-CTGGAGAGAGCCA CAGCCTA-3′ and 5′-AATGGTGCTGGGCAGGAAGT-3′. 2 μL of the first-round

PCR product was used as the template for the second-round PCR. Primers for the second-round PCR were as follows: 5′-ACAGCCTAGGGAGAGCACTG-3′ and 5′-ATGGTGCTGGGCAGGAAGTC-3′. The PCR conditions were 35 cycles at 94°C for 1 min, 58°C for 45 s, and 72°C for 1 min. The final PCR product size was 327 bp. PCR products were verified by sequencing. β-Actin was used as a control and amplified by the primers actin-L (5′-AGCCATGTACGTAGCCA TCC-3′) and actin-R (5′-CTCTCAGCTGTGGTGGTGAA-3′). The PCR product size was 226 bp. WT splenocytes stimulated with LPS (50 μg/mL) and human transforming growth factor β (hTGFβ) (1 ng/mL) for 48 hr were used as a positive control, and splenocytes or thymic B cells from AID$^{-/-}$ mice were used as a negative control for the detection of circle transcripts.

High-Throughput Sequencing Library Generation

For the 3H9 class-switched versus unswitched cells from the thymus, single-cell thymic preps were depleted of CD4$^+$ and CD8$^+$ cells using EasySep mouse streptavidin rapidspheres (STEMCELL Technologies) and sorted using a FACSAria for CD19$^+$B220$^+$IgM$^+$IgD$^+$ or CD19$^+$B220$^+$IgM$^-$IgD$^-$ cells to >99% purity. Because of the low number of cells recovered from these sorts, each sample was mixed with 10^6 Rag$^{-/-}$ splenocytes as a carrier for RNA isolation. Rag$^{-/-}$ splenocytes alone were processed concurrently with samples to confirm that no rearrangements were amplified from this source. Two rounds of amplification were used to generate the high-throughput sequencing library: the first to amplify all Igκ genes using primers Igκ Forward (Wang et al., 2000; 5′-agacgtgtgctcttccgatcGAYATTGTGMTSACMCARWCTMCA) and Cκ reverse (5′- acacgacgctcttccgatctGGATACAGTTGGTGCAGCATC), where uppercase bases denote sequences that are complementary to the V region and constant region and lowercase bases indicate homology to primers used in the second round. The first round was amplified for ten cycles, and then this product was used to prime a second-round PCR with primers to add the required adapters and barcodes for the Illumina platform (universal forward, 5′-AATGATACGGCGACCACCGAGATCTACACTCTTTCCCTA CACGACGCTCTTCCGATCT; index reverse, 5′-CAAGCAGAAGACGGCATAC GAGATNNNNNNGTGACTGGAGTTCAGACGTGTGCTCTTCCGATC, where NNNNNN is a unique 6-bp barcode for each sample). This second-round PCR was amplified for 20 cycles. PCR products were gel-purified, mixed at equimolar ratios, and submitted to the University of Chicago Functional Genomics Facility for quality control and sequencing on the Illumina HiSeq (1 × 150 bp).

High-Throughput Sequencing Data Analysis

Data were received from the Functional Genomics Core Facility as FastQ files. Sequences with a Phred score greater than 30 at all bases were selected and filtered using the Galaxy platform (http://usegalaxy.org) and processed using the International ImMunoGeneTics information system (IMGT) High V-Quest platform, which identified the V gene, J gene, and CDR3 sequence for each read (Brochet et al., 2008). Subsequent analysis was performed using lab-generated python scripts to parse the IMGT files and generate a table reporting the usage of each functional, in-frame V-J-CDR3 combination across all samples.

To quantify repertoire abundances, raw read counts were converted to counts per million (cpm) to normalize reads between samples with different sequencing depths. Only unique V-J-CDR3 amino acid combinations that comprised at least 0.1% of the total counts in any sample were included in the principal components analysis (PCA). For PCA, cpm values were log2-scaled using a zero offset of 1e3 cpm.

Morisita-Horn dissimilarity index values were calculated based on raw read counts using the [vegdist] package in R (v[3.1.2]). The Morisita-Horn dissimilarity index measures the degree of alignment between population proportion vectors by calculating their geometric cosine angle normalized by the sum of their individual Simpson diversities. Again, we computed this statistic only for V-J-CDR3 amino acid combinations with at least 0.1% abundance in any sample.

Cloning of Full-Length Antibody cDNAs and In Vitro Antibody Production

From a list of the most abundant V-J-CDR3 combinations (those making up more than 1% of reads in a single sample), primers were designed based on homology to their V and J gene, and they were amplified from the cDNA source from which they were most abundant. Following cloning and full-length sequence confirmation, light chains matching V-J-CDR3 combinations of interest were co-transfected alongside the 3H9 heavy chain in 293A cells for expression.

Mutation Analysis of Light Chains of Germinal Center B Cells

About 10,000 CD19$^+$GL7$^+$Fas$^+$ germinal center B cells from mesenteric lymph nodes of individual 3H9 transgenic mice were sorted. Sorted germinal center B cells were mixed with 5 × 10^6 splenocytes from Rag$^{-/-}$ mice to facilitate the purification and yield of total RNA. 100 ng RNA was reverse-transcribed with oligo-dT to generate cDNA. Light chains were amplified from cDNA using the Igκ forward and Cκ reverse primers described above. The PCR products were ligated into the pCR2.1 vector, and individual clones were sequenced.

Antibody Specificity Testing

Antibody concentrations in transfection supernatants were determined by ELISA, and supernatants were used to stain HEP-2 slides (MBL International). Images were acquired using a Leica DMRB on a 63× oil objective at room temperature using a Qimaging Retiga 2000R camera with Q Capture Pro software. Using ImageJ, the intensity of signal in the GFP channel was quantified in regions that were DAPI$^+$ and was normalized as the relative intensity between the ANA-positive control and untransfected supernatant-negative control for each antibody.

T Cell Adoptive Transfer

Total splenocytes from B6 or AID$^{-/-}$ mice were first labeled with 2.5 μM CFSE for 5 min at 37°C, after which CD4$^+$ T cells were enriched by positive selection on AutoMACS (Miltenyi) to more than 90% purity. 5 × 10^6 CFSE-labeled CD4$^+$ T cells were injected i.v. into B6.CD45.1 recipients. After 7 days, transferred T cells were identified by congenic marker, and CFSE dilution and Tfh cells were assessed.

Statistical Analysis

Statistical analysis was performed using Prism (GraphPad). Unless pairwise analysis is noted in the figure legend, all t tests were performed as unpaired Student's t test. *$p < 0.05$, **$p < 0.01$, ***$p < 0.001$.

ACCESSION NUMBERS

The series accession number for the data reported in this paper is NCBI GEO: GSE85366.

SUPPLEMENTAL INFORMATION

Supplemental Information includes one figure and can be found with this article online at http://dx.doi.org/10.1016/j.celrep.2016.09.011.

AUTHOR CONTRIBUTIONS

J.P., M.W., and H.H. designed the project and conceived the hypotheses. J.P., Z.Z., S.L., D.Y., and K.E.B. conducted the experiments. J.P., Z.Z., S.L., H.G., O.K., J.I.C.B., Y.L., A.S.C., A.R.D., M.W., and H.H. analyzed data and interpreted the experimental results. J.P., Z.Z., and H.H. wrote the manuscript.

ACKNOWLEDGMENTS

We thank Drs. Tasuku Honjo and Rafael Casellas for providing the AID$^{-/-}$ mice; Drs. Michael Reth and John Cambier for providing the Mb1-cre mice; Dr. Peter Savage for providing the AIRE$^{-/-}$ mice; Dr. Dominik Schenten for advice on circle transcripts; Crystal Rayon, Ashley Arthur, Douglas Kline, and Justin Kline for help with mice; and the University of Chicago Functional Genomics Core Facility, Flow Cytometry Core Facility, and Light Microscopy Core Facility. This work was supported by NIH/National Institute of Allergy and Infectious Diseases (NIAID) Grant R01 AI087645 (to H.H.). J.P. was partially supported by NIH/NIAID grant 2T32AI007090.

Received: November 18, 2015
Revised: July 20, 2016
Accepted: September 2, 2016
Published: October 4, 2016

REFERENCES

Akashi, K., Richie, L.I., Miyamoto, T., Carr, W.H., and Weissman, I.L. (2000). B lymphopoiesis in the thymus. J. Immunol. *164*, 5221–5226.

Anderson, M.S., Venanzi, E.S., Klein, L., Chen, Z., Berzins, S.P., Turley, S.J., von Boehmer, H., Bronson, R., Dierich, A., Benoist, C., and Mathis, D. (2002). Projection of an immunological self shadow within the thymus by the aire protein. Science *298*, 1395–1401.

Barnden, M.J., Allison, J., Heath, W.R., and Carbone, F.R. (1998). Defective TCR expression in transgenic mice constructed using cDNA-based alpha- and beta-chain genes under the control of heterologous regulatory elements. Immunol. Cell Biol. *76*, 34–40.

Brard, F., Shannon, M., Prak, E.L., Litwin, S., and Weigert, M. (1999). Somatic mutation and light chain rearrangement generate autoimmunity in anti-single-stranded DNA transgenic MRL/lpr mice. J. Exp. Med. *190*, 691–704.

Brochet, X., Lefranc, M.-P., and Giudicelli, V. (2008). IMGT/V-QUEST: the highly customized and integrated system for IG and TR standardized V-J and V-D-J sequence analysis. Nucleic Acids Res. *36*, W503-8.

Casciola-Rosen, L.A., Anhalt, G., and Rosén, A. (1994). Autoantigens targeted in systemic lupus erythematosus are clustered in two populations of surface structures on apoptotic keratinocytes. J. Exp. Med. *179*, 1317–1330.

Chen, C., Nagy, Z., Prak, E.L., and Weigert, M. (1995). Immunoglobulin heavy chain gene replacement: a mechanism of receptor editing. Immunity *3*, 747–755.

Chen, C., Li, H., Tian, Q., Beardall, M., Xu, Y., Casanova, N., and Weigert, M. (2006). Selection of anti-double-stranded DNA B cells in autoimmune MRL-lpr/lpr mice. J. Immunol. *176*, 5183–5190.

Chen, L., Guo, L., Tian, J., Zheng, B., and Han, S. (2010). Deficiency in activation-induced cytidine deaminase promotes systemic autoimmunity in lpr mice on a C57BL/6 background. Clin. Exp. Immunol. *159*, 169–175.

Cocca, B.A., Seal, S.N., D'Agnillo, P., Mueller, Y.M., Katsikis, P.D., Rauch, J., Weigert, M., and Radic, M.Z. (2001). Structural basis for autoantibody recognition of phosphatidylserine-beta 2 glycoprotein I and apoptotic cells. Proc. Natl. Acad. Sci. USA *98*, 13826–13831.

Crouch, E.E., Li, Z., Takizawa, M., Fichtner-Feigl, S., Gourzi, P., Montaño, C., Feigenbaum, L., Wilson, P., Janz, S., Papavasiliou, F.N., and Casellas, R. (2007). Regulation of AID expression in the immune response. J. Exp. Med. *204*, 1145–1156.

Davidson, H.W., and Watts, C. (1989). Epitope-directed processing of specific antigen by B lymphocytes. J. Cell Biol. *109*, 85–92.

Desanti, G.E., Cowan, J.E., Baik, S., Parnell, S.M., White, A.J., Penninger, J.M., Lane, P.J.L., Jenkinson, E.J., Jenkinson, W.E., and Anderson, G. (2012). Developmentally regulated availability of RANKL and CD40 ligand reveals distinct mechanisms of fetal and adult cross-talk in the thymus medulla. J. Immunol. *189*, 5519–5526.

Detanico, T., Heiser, R.A., Aviszus, K., Bonorino, C., and Wysocki, L.J. (2011). Self-tolerance checkpoints in CD4 T cells specific for a peptide derived from the B cell antigen receptor. J. Immunol. *187*, 82–91.

Dongre, A.R., Kovats, S., deRoos, P., McCormack, A.L., Nakagawa, T., Paharkova-Vatchkova, V., Eng, J., Caldwell, H., Yates, J.R., 3rd, and Rudensky, A.Y. (2001). In vivo MHC class II presentation of cytosolic proteins revealed by rapid automated tandem mass spectrometry and functional analyses. Eur. J. Immunol. *31*, 1485–1494.

Ferrero, I., Anjuère, F., Martín, P., Martínez del Hoyo, G., Fraga, M.L., Wright, N., Varona, R., Márquez, G., and Ardavín, C. (1999). Functional and phenotypic analysis of thymic B cells: role in the induction of T cell negative selection. Eur. J. Immunol. *29*, 1598–1609.

Fujihara, C., Williams, J.A., Watanabe, M., Jeon, H., Sharrow, S.O., and Hodes, R.J. (2014). T cell-B cell thymic cross-talk: maintenance and function of thymic B cells requires cognate CD40-CD40 ligand interaction. J. Immunol. *193*, 5534–5544.

Gay, D., Saunders, T., Camper, S., and Weigert, M. (1993). Receptor editing: an approach by autoreactive B cells to escape tolerance. J. Exp. Med. *177*, 999–1008.

Hase, K., Takahashi, D., Ebisawa, M., Kawano, S., Itoh, K., and Ohno, H. (2008). Activation-induced cytidine deaminase deficiency causes organ-specific autoimmune disease. PLoS ONE *3*, e3033.

Hashimoto, K., Joshi, S.K., and Koni, P.A. (2002). A conditional null allele of the major histocompatibility IA-beta chain gene. Genesis *32*, 152–153.

Hobeika, E., Thiemann, S., Storch, B., Jumaa, H., Nielsen, P.J., Pelanda, R., and Reth, M. (2006). Testing gene function early in the B cell lineage in mb1-cre mice. Proc. Natl. Acad. Sci. USA *103*, 13789–13794.

Inaba, M., Inaba, K., Adachi, Y., Nango, K., Ogata, H., Muramatsu, S., and Ikehara, S. (1990). Functional analyses of thymic CD5+ B cells. Responsiveness to major histocompatibility complex class II-restricted T blasts but not to lipopolysaccharide or anti-IgM plus interleukin 4. J. Exp. Med. *171*, 321–326.

Inaba, M., Inaba, K., Fukuba, Y., Mori, S., Haruna, H., Doi, H., Adachi, Y., Iwai, H., Hosaka, N., Hisha, H., et al. (1995). Activation of thymic B cells by signals of CD40 molecules plus interleukin-10. Eur. J. Immunol. *25*, 1244–1248.

Kawabe, T., Naka, T., Yoshida, K., Tanaka, T., Fujiwara, H., Suematsu, S., Yoshida, N., Kishimoto, T., and Kikutani, H. (1994). The immune responses in CD40-deficient mice: impaired immunoglobulin class switching and germinal center formation. Immunity *1*, 167–178.

Kinoshita, K., Harigai, M., Fagarasan, S., Muramatsu, M., and Honjo, T. (2001). A hallmark of active class switch recombination: transcripts directed by I promoters on looped-out circular DNAs. Proc. Natl. Acad. Sci. USA *98*, 12620–12623.

Klein, L., Kyewski, B., Allen, P.M., and Hogquist, K.A. (2014). Positive and negative selection of the T cell repertoire: what thymocytes see (and don't see). Nat. Rev. Immunol. *14*, 377–391.

Kuraoka, M., Holl, T.M., Liao, D., Womble, M., Cain, D.W., Reynolds, A.E., and Kelsoe, G. (2011). Activation-induced cytidine deaminase mediates central tolerance in B cells. Proc. Natl. Acad. Sci. USA *108*, 11560–11565.

Lanzavecchia, A. (1990). Receptor-mediated antigen uptake and its effect on antigen presentation to class II-restricted T lymphocytes. Annu. Rev. Immunol. *8*, 773–793.

Le Borgne, M., Ladi, E., Dzhagalov, I., Herzmark, P., Liao, Y.F., Chakraborty, A.K., and Robey, E.A. (2009). The impact of negative selection on thymocyte migration in the medulla. Nat. Immunol. *10*, 823–830.

Liang, Z., Chen, C., and Mohan, C. (2003). Molecular signatures of anti-nuclear antibodies: contributions of specific light chain residues and a novel New Zealand Black V kappa 1 germline gene. J. Immunol. *171*, 3886–3894.

Martin, S.W., and Goodnow, C.C. (2002). Burst-enhancing role of the IgG membrane tail as a molecular determinant of memory. Nat. Immunol. *3*, 182–188.

Meyers, G., Ng, Y.-S., Bannock, J.M., Lavoie, A., Walter, J.E., Notarangelo, L.D., Kilic, S.S., Aksu, G., Debré, M., Rieux-Laucat, F., et al. (2011). Activation-induced cytidine deaminase (AID) is required for B-cell tolerance in humans. Proc. Natl. Acad. Sci. USA *108*, 11554–11559.

Moisini, I., Huang, W., Bethunaickan, R., Sahu, R., Ricketts, P.-G., Akerman, M., Marion, T., Lesser, M., and Davidson, A. (2012). The Yaa locus and IFN-α fine-tune germinal center B cell selection in murine systemic lupus erythematosus. J. Immunol. *189*, 4305–4312.

Munthe, L.A., Corthay, A., Os, A., Zangani, M., and Bogen, B. (2005). Systemic autoimmune disease caused by autoreactive B cells that receive chronic help from Ig V region-specific T cells. J. Immunol. *175*, 2391–2400.

Muramatsu, M., Kinoshita, K., Fagarasan, S., Yamada, S., Shinkai, Y., and Honjo, T. (2000). Class switch recombination and hypermutation require activation-induced cytidine deaminase (AID), a potential RNA editing enzyme. Cell *102*, 553–563.

Ota, M., Duong, B.H., Torkamani, A., Doyle, C.M., Gavin, A.L., Ota, T., and Nemazee, D. (2010). Regulation of the B cell receptor repertoire and self-reactivity by BAFF. J. Immunol. *185*, 4128–4136.

Pape, K.A., Catron, D.M., Itano, A.A., and Jenkins, M.K. (2007). The humoral immune response is initiated in lymph nodes by B cells that acquire soluble antigen directly in the follicles. Immunity *26*, 491–502.

Perera, J., and Huang, H. (2015). The development and function of thymic B cells. Cell. Mol. Life Sci. *72*, 2657–2663.

Perera, J., Meng, L., Meng, F., and Huang, H. (2013). Autoreactive thymic B cells are efficient antigen-presenting cells of cognate self-antigens for T cell negative selection. Proc. Natl. Acad. Sci. USA *110*, 17011–17016.

Radic, M.Z., Mascelli, M.A., Erikson, J., Shan, H., and Weigert, M. (1991). Ig H and L chain contributions to autoimmune specificities. J. Immunol. *146*, 176–182.

Radic, M., Marion, T., and Monestier, M. (2004). Nucleosomes are exposed at the cell surface in apoptosis. J. Immunol. *172*, 6692–6700.

Roark, J.H., Kuntz, C.L., Nguyen, K.A., Caton, A.J., and Erikson, J. (1995). Breakdown of B cell tolerance in a mouse model of systemic lupus erythematosus. J. Exp. Med. *181*, 1157–1167.

Rudensky, A.Y., Mazel, S.M., and Yurin, V.L. (1990). Presentation of endogenous immunoglobulin determinant to immunoglobulin-recognizing T cell clones by the thymic cells. Eur. J. Immunol. *20*, 2235–2239.

Stavnezer, J., Guikema, J.E.J., and Schrader, C.E. (2008). Mechanism and regulation of class switch recombination. Annu. Rev. Immunol. *26*, 261–292.

Tillman, D.M., Jou, N.T., Hill, R.J., and Marion, T.N. (1992). Both IgM and IgG anti-DNA antibodies are the products of clonally selective B cell stimulation in (NZB x NZW)F1 mice. J. Exp. Med. *176*, 761–779.

Victora, G.D., Schwickert, T.A., Fooksman, D.R., Kamphorst, A.O., Meyer-Hermann, M., Dustin, M.L., and Nussenzweig, M.C. (2010). Germinal center dynamics revealed by multiphoton microscopy with a photoactivatable fluorescent reporter. Cell *143*, 592–605.

Victora, G.D., Dominguez-Sola, D., Holmes, A.B., Deroubaix, S., Dalla-Favera, R., and Nussenzweig, M.C. (2012). Identification of human germinal center light and dark zone cells and their relationship to human B-cell lymphomas. Blood *120*, 2240–2248.

Wang, Z., Raifu, M., Howard, M., Smith, L., Hansen, D., Goldsby, R., and Ratner, D. (2000). Universal PCR amplification of mouse immunoglobulin gene variable regions: the design of degenerate primers and an assessment of the effect of DNA polymerase 3′ to 5′ exonuclease activity. J. Immunol. Methods *233*, 167–177.

Watts, C. (1997). Capture and processing of exogenous antigens for presentation on MHC molecules. Annu. Rev. Immunol. *15*, 821–850.

Xu, Z., Zan, H., Pone, E.J., Mai, T., and Casali, P. (2012). Immunoglobulin class-switch DNA recombination: induction, targeting and beyond. Nat. Rev. Immunol. *12*, 517–531.

Yamano, T., Nedjic, J., Hinterberger, M., Steinert, M., Koser, S., Pinto, S., Gerdes, N., Lutgens, E., Ishimaru, N., Busslinger, M., et al. (2015). Thymic B Cells Are Licensed to Present Self Antigens for Central T Cell Tolerance Induction. Immunity *42*, 1048–1061.

Yuseff, M.-I., Pierobon, P., Reversat, A., and Lennon-Duménil, A.-M. (2013). How B cells capture, process and present antigens: a crucial role for cell polarity. Nat. Rev. Immunol. *13*, 475–486.